Responses of Mouse Airway Epithelial Cells and Alveolar Macrophages to Virulent and Avirulent Strains of Influenza A Virus

Michelle D. Tate,[1] Heidi C. Schilter,[2] Andrew G. Brooks,[1] and Patrick C. Reading[1,3]

Abstract

Influenza A virus (IAV) infection is associated with outcomes ranging from subclinical infection to severe pneumonia. In this study, we compared IAV strains BJx109 (H3N2), HKx31 (H3N2), and PR8 (H1N1), for their ability to elicit innate immune responses from mouse airway cells *in vitro* and their virulence in mice. The viruses differed markedly in their ability to induce disease in mice (PR8 > HKx31 > BJx109). In particular, PR8 infection was associated with high levels of virus replication and pulmonary inflammation. We next compared the ability of each virus strain to infect and induce inflammatory mediators from mouse airway cells. First, major differences were observed in the ability of viruses to infect and induce chemokines and cytokines from mouse alveolar macrophages (BJx109 > HKx31 > PR8), but not from airway epithelial cells (AEC) *in vitro*. Second, C-type lectins of the innate immune system in mouse lung fluids blocked the ability of BJx109, but not PR8, to infect mouse macrophages and AEC. The failure of the virulent PR8 virus to elicit responses from airway macrophages, combined with resistance to antiviral proteins in mouse airway fluids, likely contribute to virulence in mice. These findings provide insight into the mechanisms underlying disease severity in the mouse model of influenza infection.

Introduction

INFLUENZA A VIRUSES (IAV) INFECT CELLS LINING THE RESPIRATORY TRACT, namely bronchiolar-alveolar epithelial cells and alveolar macrophages (MΦ). Following entry into epithelial cells, IAV replicates productively and buds from the cell surface to facilitate infection and spread throughout the airways. IAV also infects alveolar MΦ (23,44,65); however, these cells contribute to host defense rather than disease, by virtue of their inability to support productive virus replication (48,65). In addition, MΦ phagocytose virions and virus-infected cells (16,21), and respond to virus via the production of proinflammatory chemokines and cytokines (24,43,51). Depletion of airway MΦ with clodronate-loaded liposomes has been associated with enhanced virus replication and disease in mice (59,61,66), and pigs (30).

Respiratory tract secretions contain a range of antimicrobial proteins and peptides, some of which mediate antiviral activity against IAV. In particular, surfactant protein (SP)-A and SP-D are large, oligomeric proteins of the collectin family that mediate a range of antiviral activities [reviewed in (12)]. SP-D binds in a Ca^{2+}-depedent manner to mannose-rich glycans on the hemagglutinin (HA) and neuraminidase (NA) glycoproteins (18,20,45), whereas SP-A inhibits virus independently of calcium, acting as a sialylated γ-inhibitor that competes with cell-surface receptors for binding to the viral HA (4). The enhanced susceptibility of SP-D knockout mice to infection with highly glycosylated strains of influenza A virus highlights the important role of SP-D in innate immune defense against IAV *in vivo* (22,34,63). SP-A knockout mice were also more susceptible to IAV; however, the difference was not as striking as that observed in SP-D-deficient mice (33,35).

Different cell types in the lung produce differing spectrums of cytokines and chemokines following exposure to IAV. *In vitro* studies using human cells showed that IAV-infected epithelial cells are relatively poor producers of type 1 interferons (IFN) and proinflammatory cytokines, whereas

[1]Department of Microbiology and Immunology, University of Melbourne, Victoria, Australia.
[2]Garvan Institute of Medical Research, Sydney, New South Wales, Australia.
[3]WHO Collaborating Centre for Reference and Research on Influenza, Victorian Infectious Diseases Reference Laboratory, North Melbourne, Victoria, Australia.

monocytes/MΦ produce large quantities of these mediators (29,49). Furthermore, infection of lung epithelial cells favored production of IL-8 and other neutrophil-attracting chemokines (2,29), whereas human monocytes/MΦ produce inflammatory mediators that attract mononuclear leukocytes and suppress neutrophil-attracting chemokines (54). Therefore, the tropism of a particular virus strain for cells of the human respiratory tract is likely to determine the spectrum of chemoattractants produced in the lung.

Despite interest in the interactions of IAV with human epithelial cells and MΦ *in vitro* (2,7,9,25,29,36,49,54), few studies have addressed their murine counterparts. The mouse model of influenza infection also allows in vitro responses of airway cells to be correlated with virulence *in vivo*. We have demonstrated that mouse-adapted A/PR/8/34 (PR8; H1N1) infects mouse MΦ poorly and is highly virulent in mice (44,45,59). Depletion of airway MΦ has been associated with exacerbated disease (30,59,61,66); however, PR8 infection was not affected (59), indicating that a poor ability to infect airway MΦ could be an important factor contributing to the virulence of PR8 in mice. Sensitivity to innate proteins in lung fluids could further modify the ability of virus to infect and induce inflammatory mediators from airway cells. Herein, we compared PR8 (H1N1) with HKx31 (H3N2) and BJx109 (H3N2), which are reassortant viruses bearing internal components derived from PR8, in conjunction with HA and NA from A/Aichi/2/68 (H3N2) and A/Beijing/353/89 (H3N2), respectively. The three viruses were compared for (1) their ability to infect and induce inflammatory mediators from primary airway epithelial cells (AEC) and alveolar MΦ *in vitro*, (2) their sensitivity to neutralization by innate immune proteins in mouse airway fluids, and (3) their ability to induce cytokines and chemokines, inflammation, and disease in mice following intranasal inoculation. The virulence of the PR8 strain correlated with its ability to evade both soluble and cellular components of innate immune defense.

Materials and Methods

Mice and viruses

C57BL/6 (B6) mice and B6.RAG-1$^{-/-}$ mice were bred and housed in specific pathogen-free conditions at the Department of Microbiology and Immunology, University of Melbourne. Male mice 6–8 wk of age were used in all experiments. B6.RAG-1$^{-/-}$ mice lack mature T- and B-cell populations due to a mutation in the recombination activation gene (RAG)-1 gene (37). The IAV strains used in this study were A/PR/8/34 (PR8, H1N1), HKx31 (H3N2), and BJx109 (H3N2). HKx31 and BJx109 are high-yield reassortants of PR8 with A/Aichi/2/68 (H3N2) and A/Beijing/353/89 (H3N2), respectively, and bear the H3N2 surface glycoproteins. The viruses were grown in 10-day embryonated eggs by standard procedures and titrated on Madin-Darby canine kidney (MDCK) cells, as previously described (1).

Preparation and infection of mouse airway MΦ and epithelial cells

Mouse airway MΦ were recovered via bronchoalveolar lavage (BAL) of naïve mice, as previously described (44). Mouse AEC cultures, consisting of alveolar type I and II cells and bronchial epithelial cells, were prepared as previously described (13,15,50), with minor modifications. Briefly, lungs were excised and placed in phosphate-buffered saline (PBS) containing 100 U/mL penicillin/streptomycin. Excess tissue, including pleura and branching airways, were removed, and lungs from four mice were diced and placed in a 15-mL flask, with dissociation medium (DMEM:Ham's F-12; Invitrogen Corp., Carlsbad, CA), 1.5 mg/mL Pronase (Roche Diagnostics Corp., Indianapolis, IN), and 0.1 mg/mL DNAse I (Sigma-Aldrich, St. Louis, MO), and incubated at 37°C in 5% CO_2 for 60 min. The flasks were inverted 12 times, and the contents were placed on a 70-μm filter, and cells were strained with 10 mL DMEM:Ham's F-12, supplemented with 5% fetal calf serum, 2 mM L-glutamine, 100 U/mL penicillin and streptomycin, and 120 IU/L human insulin (Novo Nordisk, Bagsværd, Denmark; DMEM/F-12$_5$). The cells were cultured in DMEM/F-12$_5$ in either 24-well plates, culture flasks, or 8-well chamber slides pre-coated with Matrigel (BD Biosciences, San Jose, CA). Cell purity was typically >99% as assessed by staining cells grown on glass cover-slips with anti-cytokeratin and anti-E-cadherin antibodies (Santa Cruz Biotechnology, Santa Cruz, CA). LA-4 cells, a mouse respiratory epithelial cell line, was also used in some experiments, as indicated.

BAL MΦ (2.5×10^5 cells/well) or AEC (3×10^4 cells/well) were seeded into 8-well glass chamber slides, such that similar cell densities were obtained following overnight incubation at 37°C in 5% CO_2. Cell monolayers were washed with serum-free medium and infected with 10^6 plaque-forming units (PFU) of IAV, as previously described (44). At 8 h post-infection, the slides were washed in PBS, fixed in 80% vol/vol acetone, and stained with mAb MP3.10g2.IC7 (WHO Collaborating Centre for Reference and Research on Influenza, Melbourne, Australia), which is specific for the nucleoprotein of IAV, followed by fluorescein isothiocyanate (FITC)-conjugated sheep anti-mouse immunoglobulin (Silenus, Melbourne, Australia), and viewed under 40×magnifi-magnification. The percentage of fluorescent cells was determined in a minimum of four random fields, with a minimum of 200 cells counted for each sample.

To determine the titer of infectious virus present in supernatants from IAV-infected MΦ or AEC, monolayers were incubated with 10^6 PFU of BJx109, HKx31, or PR8 viruses for 60 min, washed three times to remove free virus, and cultured at 37°C. At 2 h and 24 h post-infection, the supernatants were removed, and the presence of infectious virus was determined by standard plaque assay on MDCK cell monolayers in the presence of trypsin (1).

To assess the ability of BAL MΦ and AEC to produce inflammatory mediators, monolayers were infected as described above, and 24 h later the cell supernatants were collected, clarified by centrifugation, and frozen at −20°C. Levels of IFN-γ, TNF-α, IL-6, MCP-1/CCL2, and RANTES/CCL5 in cell-free supernatants were determined by mouse cytokine bead array (BD Biosciences), according to the manufacturer's instructions. Inflammatory mediator concentrations were calculated using a standard curve and expressed as picograms per milliliter. Levels of murine GM-CSF, KC/CXCL1, MIP-1α/CCL3, and MIP-2/CXCL2 were determined via ELISA (Roche Diagnostics Corp.), according to the manufacturer's instructions.

Virus neutralization assay

Neutralization of IAV infectivity was measured by fluorescent-focus reduction in monolayers of MDCK cells cultured in 96-well plates, as previously described (45).

Virus infection of mice

Mice were anesthetized and infected with 10^2 or 10^5 PFU of BJx109, HKx31, or PR8, via the intranasal (IN) route in $50\,\mu L$ of PBS. The mice were weighed daily and assessed for visual signs of clinical disease, including inactivity, ruffled fur, labored breathing, and huddling behavior. Animals that had lost $\geq 25\%$ of their original body weight and/or displayed evidence of pneumonia were euthanized. All research complied with the University of Melbourne's Animal Experimentation Ethics guidelines and policies. At various time points after infection, mice were euthanized and the lungs, nasal tissues, thymus, brains, and hearts were removed, homogenized in PBS, and clarified by centrifugation. Titers of infectious virus in tissue homogenates were determined by standard plaque assay on MDCK cells.

Recovery and characterization of leukocytes from mice

BAL cells were obtained as previously described (58). Samples were treated with Tris-NH$_4$Cl (0.14 M NH$_4$Cl in 17 mM Tris, adjusted to pH 7.2) to lyse erythrocytes, and washed in RPMI-1640 medium supplemented with 10% FCS (RF$_{10}$). For flow cytometric analysis, BAL cell suspensions were incubated on ice for 20 min with supernatants from hybridoma 2.4G2 to block Fc receptors, followed by staining with appropriate combinations of FITC-, phycoerythrin (PE)-, and allophycocyanin (APC)-conjugated or biotinylated monoclonal antibodies to Gr-1 (RB6-8C5), CD45.2 (104), CD8a (53-6.7), CD4 (GK1.5), B220 (RA3-6B2), TCR-β (H57-597), and NK1.1 (PK136). Living cells were identified by the addition of $10\,\mu g/mL$ propidium iodide (PI) to each sample, and the cells were analyzed using a FACSCalibur flow cytometer. A minimum of 50,000 PI$^-$ cells were collected for each sample.

Pulmonary histopathology

Hematoxylin and eosin (H&E)-stained lung sections were randomized and scored blind for airway inflammation using a scale of 0, 1, 2, 3, 4, or 5 (corresponding to none, very mild, mild, moderate, marked, and severe inflammation, respectively) by three independent readers, as previously described (58). Tissues were graded for peribronchiolar inflammation (around 3–5 small airways per section), and alveolitis in multiple random fields per section. Lung sections were viewed with a Leica DMI3000 B microscope (Leica Microsystems, Inc., Bannockburn, IL), and photographed at $10\times$ magnification unless otherwise stated, using a Leica DFC 490 camera with the Leica Application software. Immunoperoxidase staining of paraffin-embedded lung sections to examine the distribution of viral antigens was performed as previously described (58).

Assessment of lung edema and vascular leak

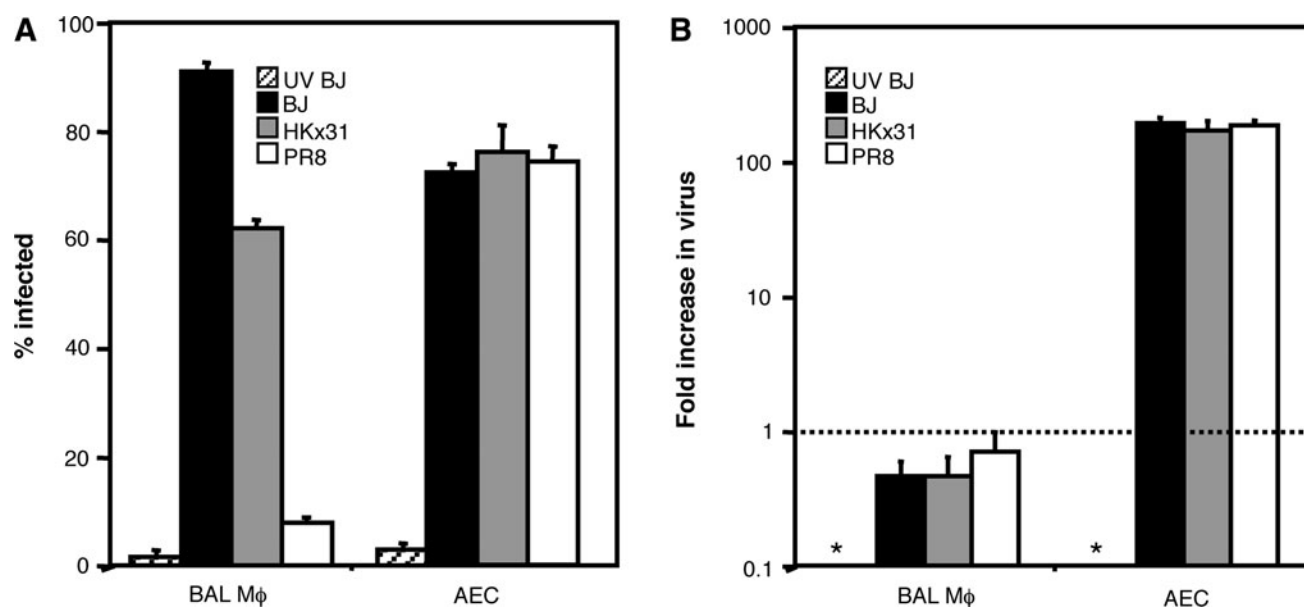The lung wet-to-dry weight ratio was used as an index of lung water accumulation during IAV infection, and was

FIG. 1. The ability of influenza virus to infect alveolar MΦ and alveolar epithelial cells (AEC) *in vitro*. Monolayers of bronchoalveolar lavage (BAL) MΦ or primary AEC were incubated with 10^6 PFU of BJx109 (BJ), HKx31, or PR8, or with an equivalent dose of BJx109 that had been UV-irradiated for 30 min to destroy virus infectivity (UV BJ). After 1 h at 37°C, the monolayers were washed and cultured in serum-free media. (**A**) At 8 h post-infection, the monolayers were fixed and stained by immunofluorescence for expression of viral NP. Data represent the mean percent infection (± 1 SD) from a minimum of four independent fields per chamber. (**B**) Supernatants were removed at 2 h and 24 h post-infection, and levels of infectious virus were determined by plaque assay on MDCK cells. Results are expressed as the fold increase in infectious virus between 2 and 24 h. Data represent the mean (± 1 SD) from three independent experiments (*a fold increase of 0.1 ± 0 was recorded for both BAL MΦ and AEC). Data are representative of five or more independent experiments.

performed as previously described (58). The concentration of protein in BAL supernatants was measured by adding Bradford protein dye. A standard curve using BSA was constructed, and the optical density (OD) determined at 595 nm.

Quantification of inflammatory mediators in bronchoalveolar lavage fluid

The levels of IL-6, GM-CSF, IFN-γ, TNF-α, KC, MCP-1, MIP-1α, MIP-1β, and RANTES in BAL supernatants from virus-infected mice were determined using the mouse cytokine 23-plex Bio-Plex assay (Bio-Rad Laboratories, Inc., Hercules, CA), according to the manufacturer's instructions. Data were collected with a minimum of 100 beads per sample analyzed using Bio-Plex Manager Software. Concentrations were calculated from a standard curve and expressed as picograms per milliliter.

Statistical analysis

For the comparison of two sets of values, a Student's t-test (two-tailed, two-sample equal variance) was used. When comparing three or more sets of values, a one-way analysis of variance (ANOVA) was applied. A p value of ≤ 0.05 was considered statistically significant.

Results

Influenza viruses infect AEC to similar levels, but differ markedly in their ability to infect alveolar MΦ

In previous reports, we have demonstrated that BJx109 infects murine macrophages efficiently, whereas PR8 does not (44,47,59). We first confirmed these observations in independent experiments using alveolar MΦ, and for comparison, primary mouse AEC. Immunofluorescence confirmed that BJx109 infected alveolar MΦ to high levels (~90%; Fig. 1A), and HKx31 infected MΦ to intermediate levels (~60%), whereas PR8 was poor in its ability to infect airway MΦ (~5–10%). In contrast, virus strains infected primary AEC to equivalent levels (~70%; Fig. 1A).

To assess the ability of IAV to replicate in mouse MΦ and epithelial cells, monolayers of BAL MΦ or AEC were inoculated with 10^6 PFU of BJx109, HKx31, or PR8, or with an equivalent dose of UV-inactivated BJx109. After 1 h, the cells were washed and fresh serum-free media was added. Supernatants were harvested 2 or 24 h after exposure to virus, and infectious virus present was determined by standard plaque assay on MDCK cells. Data are expressed as the fold increase between 2 and 24 h (Fig. 1B). Incubation of MΦ with each virus strain did not result in virus amplification, consistent with previous reports that influenza A virus infection of murine MΦ is non-productive (48,65). In contrast, infectious virus in supernatants from AEC exposed to BJx109, HKx31, or PR8 increased >100-fold between 2 and 24 h, consistent with the ability of epithelial cells to support productive virus infection (3,46).

Production of inflammatory mediators by alveolar MΦ and AECs following exposure to BJx109, HKx31, or PR8

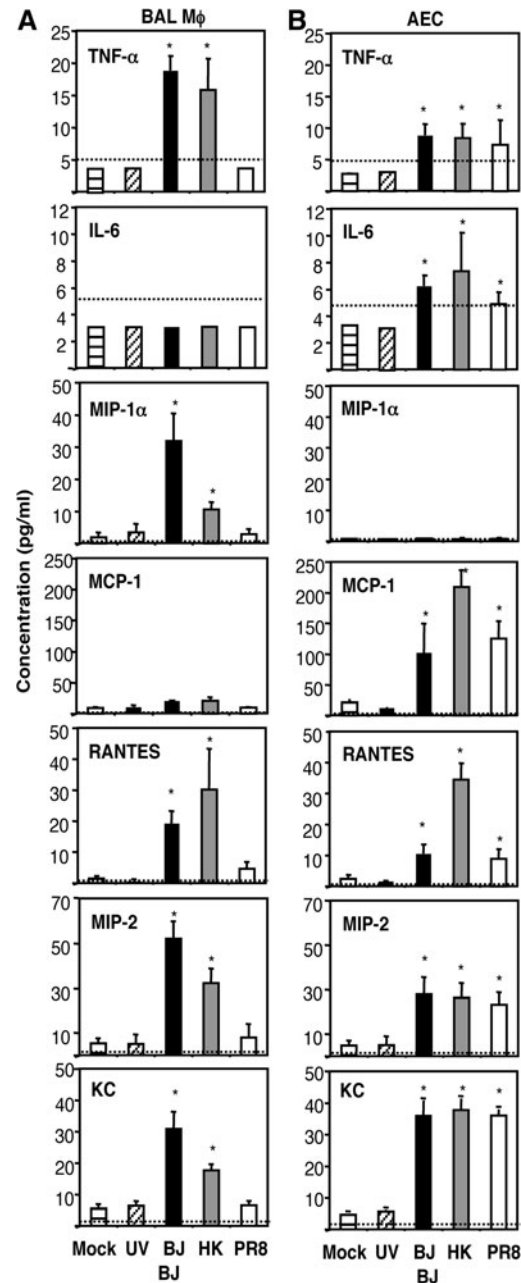Next, we determined the spectrum and levels of inflammatory mediators produced following exposure of mouse

FIG. 2. Production of inflammatory mediators by alveolar MΦ and alveolar epithelial cells (AEC) following exposure to influenza viruses. Monolayers of bronchoalveolar lavage (BAL) MΦ and AEC were incubated for 1 h at 37°C with 10^6 PFU of BJx109 (BJ), HKx31 (HK) or PR8, or with media alone (Mock). Cell monolayers were also incubated with 10^6 PFU of BJx109 that had been UV-irradiated for 30 min to destroy virus infectivity (UV BJ). The cells were washed and incubated for 24 h, and the supernatants were removed, clarified, and assayed for a range of inflammatory mediators. Cytokine/chemokine concentrations were assayed via ELISA or cytokine bead array (CBA) as described in the Materials and Methods section. Data represent the mean ± 1 SD from three independent experiments. The detection limit of each assay is indicated as a dotted line (TNF-α = 5 pg/mL, IL-6 = 5 pg/mL, MIP-1α = 2 pg/mL, MCP-1 = 5 pg/mL, RANTES = 2 pg/mL, MIP-2 = 2 pg/mL, KC = 2 pg/ml; *levels were significantly different from those in supernatants from mock-infected cells; $p < 0.05$ by one-way ANOVA).

MΦ or AEC to IAV (Fig. 2). Overall, alveolar MΦ exposed to IAV produced high levels of TNF-α, MIP-1α, RANTES, MIP-2, and KC, and low levels of MCP-1, whereas virus-infected AEC produced high levels of MCP-1, RANTES, MIP-2, and KC, and low levels of TNF-α and IL-6. Thus the overall spectrum of cytokine/chemokine production was different for mouse MΦ and epithelial cells. The viruses differed in their ability to induce cytokine and chemokine secretion from MΦ. BJx109 and HKx31 induced TNF-α, MIP-1α, RANTES, MIP-2, and KC, whereas an equivalent dose of PR8 did not. The induction of all cytokines and chemokines examined was dependent on infectious virus, as inflammatory mediators from MΦ or AEC exposed to UV-irradiated BJx109 were no different from the levels in mock-infected cells.

BJx109, HKx31, and PR8 differ in virulence in C57BL/6 mice

We hypothesized that the tropism of each virus strain for particular cells of the respiratory tract could be an important factor contributing to virulence and disease. Extending our previous studies comparing the virulence of BJx109 and PR8 in mice (59), B6 mice were inoculated via the intranasal route with 10^5 PFU (Fig. 3A) or 10^2 PFU (Fig. 3B) of BJx109, HKx31, or PR8, and disease was assessed by weight loss (Fig. 3, upper panels) and survival (Fig. 3, lower panels). Intranasal inoculation with 10^5 PFU of BJx109 did not induce significant weight loss; however, mice inoculated with an equivalent dose of HKx31 showed progressive weight loss over the first 6–7 d of infection, but all animals regained weight and survived the infection. Mice infected with 10^5 PFU of PR8 lost weight rapidly and all animals were euthanized. B6 mice infected with 10^2 PFU

of BJx109 or HKx31 did not show significant weight loss (Fig. 3B); however, all mice infected with an equivalent dose of PR8 lost weight progressively and succumbed to disease within 9–10 d. Thus, BJx109, HKx31, and PR8 display clear differences in their ability to induce disease, and may be classified as avirulent, of intermediate virulence, and highly virulent, respectively, in B6 mice.

Next, we compared virus strains for their ability to induce disease following IN inoculation of immunodeficient B6.RAG-1$^{-/-}$ mice (37). Inoculation of B6.RAG-1$^{-/-}$ mice with 10^2 (Fig. 3C) or 10^5 PFU (data not shown) BJx109 was not associated with significant weight loss or disease over a 15-d monitoring period. Immunocompetent B6 mice inoculated with 10^2 PFU of HKx31 showed no signs of weight loss (Fig. 3B, upper panel); however, all B6.RAG-1$^{-/-}$ mice inoculated with an equivalent dose lost weight (Fig. 3C, upper panel), and succumbed to disease (Fig. 3C, lower panel). B6 or B6.RAG-1$^{-/-}$ mice inoculated with 10^2 PFU of PR8 all succumbed to disease (Fig. 3C, lower panel), although PR8-infected B6.RAG-1$^{-/-}$ mice lost weight more rapidly and were euthanized earlier than B6 mice (Fig. 3C, upper panel). Thus, adaptive immunity is not required to restrict the ability of BJx109 to induce disease in B6 mice.

Viral replication and pulmonary inflammation following intranasal infection of B6 mice with BJx109, HKx31, or PR8

B6 mice were infected with 10^5 PFU of BJx109, HKx31, and PR8, and viral loads in the lower (lungs) and upper (nasal tissues) respiratory tract were examined at days 1–9
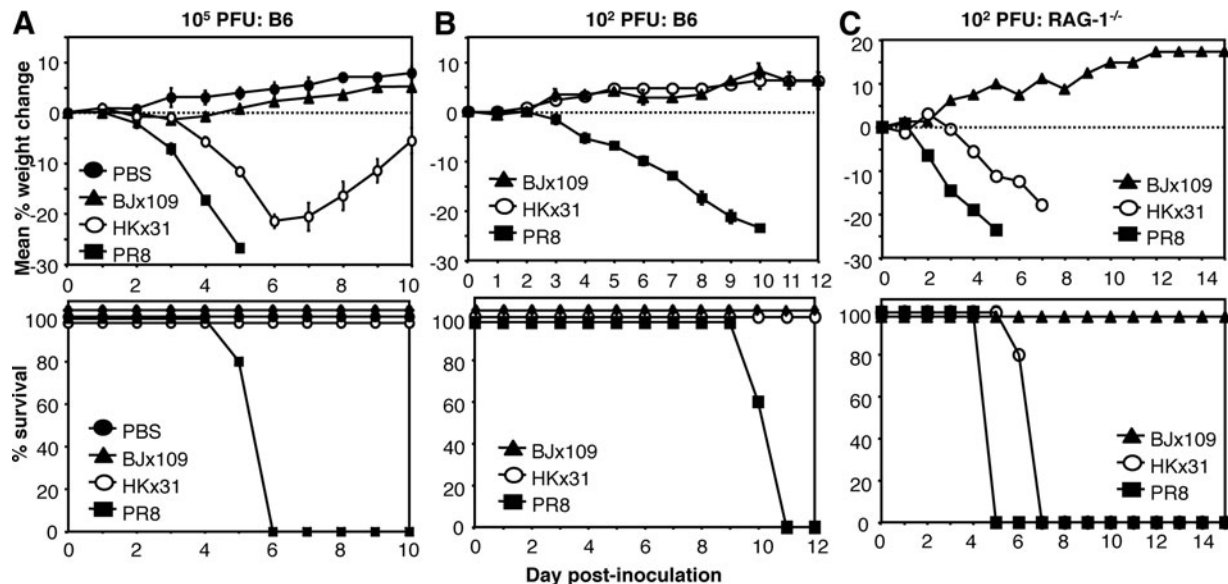

FIG. 3. Virulence of influenza strains BJx109, HKx31, and PR8 for B6 mice. Groups of five C57BL/6 (B6) mice were infected via the intranasal route with (**A**) 10^5 PFU, or (**B**) 10^2 PFU, of BJx109, HKx31, or PR8, and (**C**) B6.RAG-1$^{-/-}$ (RAG-1$^{-/-}$) mice were infected with 10^2 PFU BJx109, HKx31, or PR8. Control mice received virus diluent alone (PBS). The mice were assessed daily for weight loss (upper panels) and survival (lower panels). Mice displaying evidence of pneumonia and/or having lost ≥25% of their original body weight were euthanized. Weight loss data are expressed as the mean percent weight change of each group ± 1 SEM, compared to the weight immediately prior to infection. Data shown are from one experiment and are representative of three independent experiments.

post-infection (Fig. 4). Viral titers in the lungs (Fig. 4A) and nasal tissues (Fig. 4B) of mice infected with BJx109 virus peaked 1 d after infection, and were below the level of detection by day 5, consistent with containment of virus via the innate immune system. HKx31 replicated to substantial levels in the lungs at 1–5 d post-infection, but titers were markedly reduced 7–9 d post-infection. Viral titers were high 1 d after PR8 infection, and remained so at 3 and 5 d post-infection, when the mice were euthanized due to excessive weight loss and disease (Fig. 3).

HKx31 and PR8 showed marked differences in their pattern of replication in the lung; however, both viruses replicated to similar levels in nasal tissues at days 1, 3, and 5 post-infection (Fig. 4B). As BJx109, HKx31, and PR8 were equally efficient in their ability to replicate productively in primary AEC (Fig. 1B), differences in virus titers are likely to reflect differences in sensitivity to components of innate host defense. Moreover, we have previously shown that BJx109 can replicate to high titers ($>4.0 \log_{10}$ PFU/lung) in the lungs of mice following depletion of airway MΦ (59), demon-
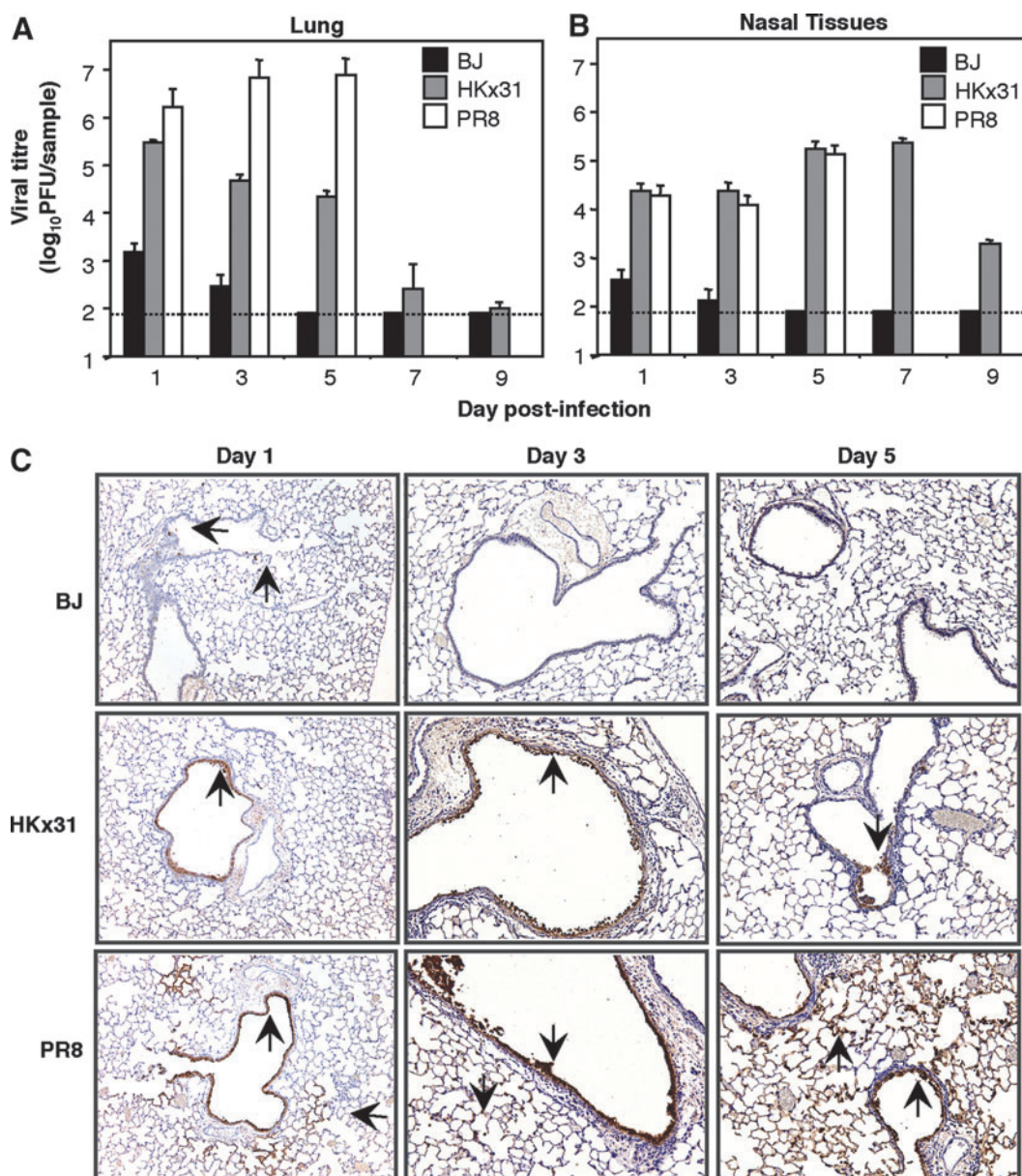

FIG. 4. Virus titers in the respiratory tract of B6 mice infected with BJx109 (BJ), HKx31, or PR8. Groups of five B6 mice were infected via the IN route with 10^5 PFU BJx109, HKx31, and PR8. Mice were euthanized and analyzed at days 1, 3, and 5 post-infection. (**A**) Lungs and (**B**) nasal tissues were homogenized and virus titers were determined by plaque assay on MDCK cells. Error bars represent the mean viral titer of each group ± 1 SD. The detection limit for the plaque assay is indicated by the dotted line. (**C**) Distribution of viral antigen in the lungs of influenza-infected mice. Cells positive for viral antigen are stained brown, and arrows indicate areas of intense antigen staining. Representative images are shown at 10×magnification. Results are representative of three independent experiments. Color images available online at www.liebertonline.com/vim.

strating that this strain can grow efficiently in the lung in the absence of specific innate defenses.

Immunoperoxidase staining of lung sections from virus-infected animals was performed to determine the distribution of viral antigen 1, 3, and 5 days after IN infection with IAV. Occasional cells staining positive for viral antigen were detected in the lungs of BJx109-infected mice at day 1 post-infection, but not at day 3 or 5 (Fig. 4C, upper panels), consistent with the low titers of infectious virus recovered from the lungs of these animals (Fig. 4A). Following infection with HKx31, viral antigen localized to epithelial cells lining the bronchioles and small airways at 1, 3, and 5 d post-infection (Fig. 4C, middle panels). Epithelial cells lining the bronchioles and small airways of PR8-infected mice stained strongly for viral antigen at days 1, 3, and 5 post-infection (Fig. 4C, lower panels), with increasing involvement of epithelial cells lining the alveolar compartments at the latter time points. By day 5 post-infection, cells stained strongly for viral antigen throughout the airways and alveoli of PR8-infected mice.

The severe clinical disease observed following infection with PR8 was characterized by enhanced recruitment of in-flammatory cells to the airways (Fig. 5A), particularly neutrophils, NK cells, T cells, and B cells (Fig. 5B). Moreover, PR8 infection resulted in lung injury, characterized by increased vascular leakage (Fig. 5C), and pulmonary edema (Fig. 5D), compared to naïve animals or to animals infected with BJx109 or HKx31.

Levels of cytokines and chemokines in BAL supernatants following infection with BJx109, HKx31, and PR8

The magnitude and nature of the cellular infiltrate in the airways and/or the production of local immunomodulators could be critical factors contributing to morbidity and mortality during IAV infection. Therefore we determined levels of cytokines and chemokines in BAL supernatants from virus-infected mice at 1, 3, and 5 days post-infection (Fig. 6). Levels of TNF-α, IL-6, MIP-1α, MCP-1, RANTES, and KC were below the level of detection in BAL supernatants of BJx109-infected mice at all time points tested, although low levels of MIP-2 were recorded at all times. In contrast, HKx31 and PR8 induced significant levels of a range
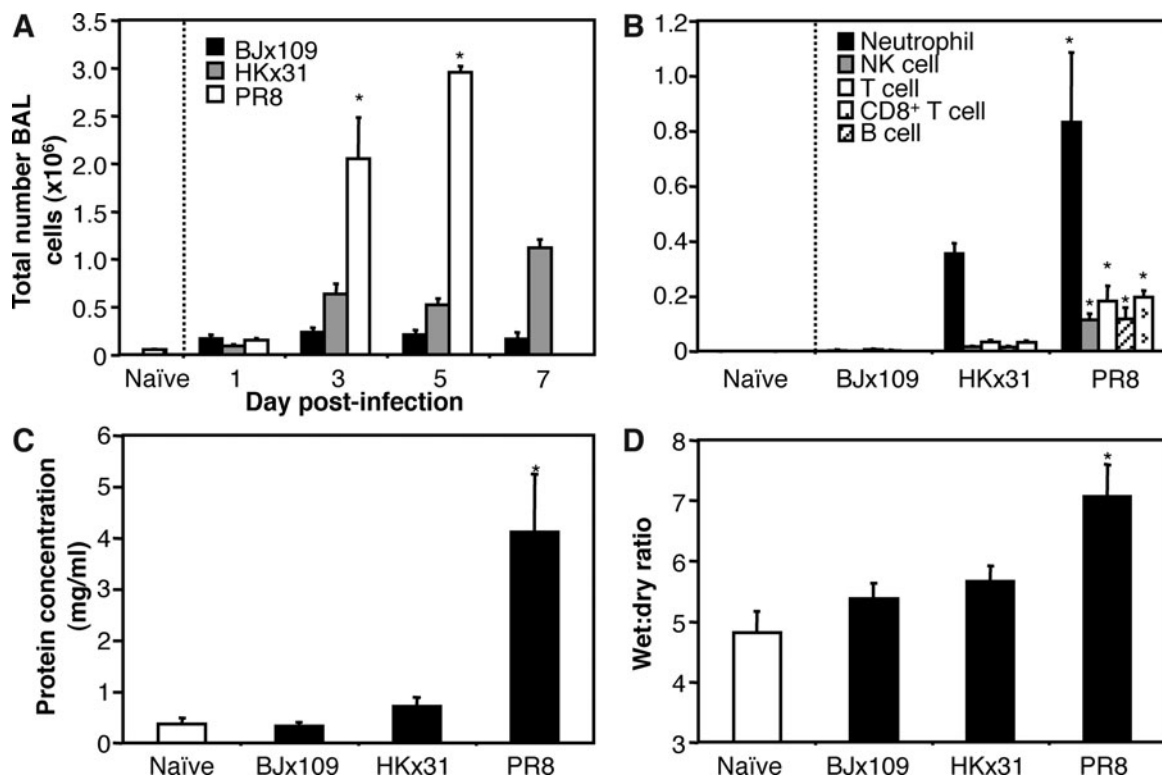

FIG. 5. Severe disease during PR8 infection of B6 mice is associated with increased inflammation and pulmonary edema. Groups of five B6 mice were infected with 10^5 PFU of BJx109, HKx31, or PR8. (**A**) At days 1–7 post-infection, the mice were euthanized and BAL performed. Total cell numbers in BAL fluid were determined and data are expressed as the mean cell number ± 1 SD (*significantly different from naïve, BJx109-, and HKx31-infected animals; $p < 0.05$ by one-way ANOVA). (**B**) At day 5 post-infection, BAL cells were recovered and examined by flow cytometry for neutrophils (Gr-1^{high}), NK cells (NK1.1$^+$ TCRβ^-), T cells (TCRβ^+), CD8$^+$ T cells (CD8$^+$ TCRβ^+), and B cells (B220$^+$). Bars represent the mean cell number ± 1 SD (*significantly different from naïve, BJx109-, and HKx31-infected mice; $p < 0.01$ by one-way ANOVA). (**C**) Total protein concentration in cell-free BAL supernatants at day 5 post-infection. Data represent the mean protein concentration ± 1 SD (*significantly different from naïve, BJx109-, and HKx31-infected animals; $p < 0.01$ by one-way ANOVA). (**D**) Lung wet:dry ratios as an assessment of pulmonary edema at day 5 post-infection (*significantly different from naïve, BJx109-, and HKx31-infected animals; $p < 0.01$ by one-way ANOVA). Results are representative of two independent experiments.
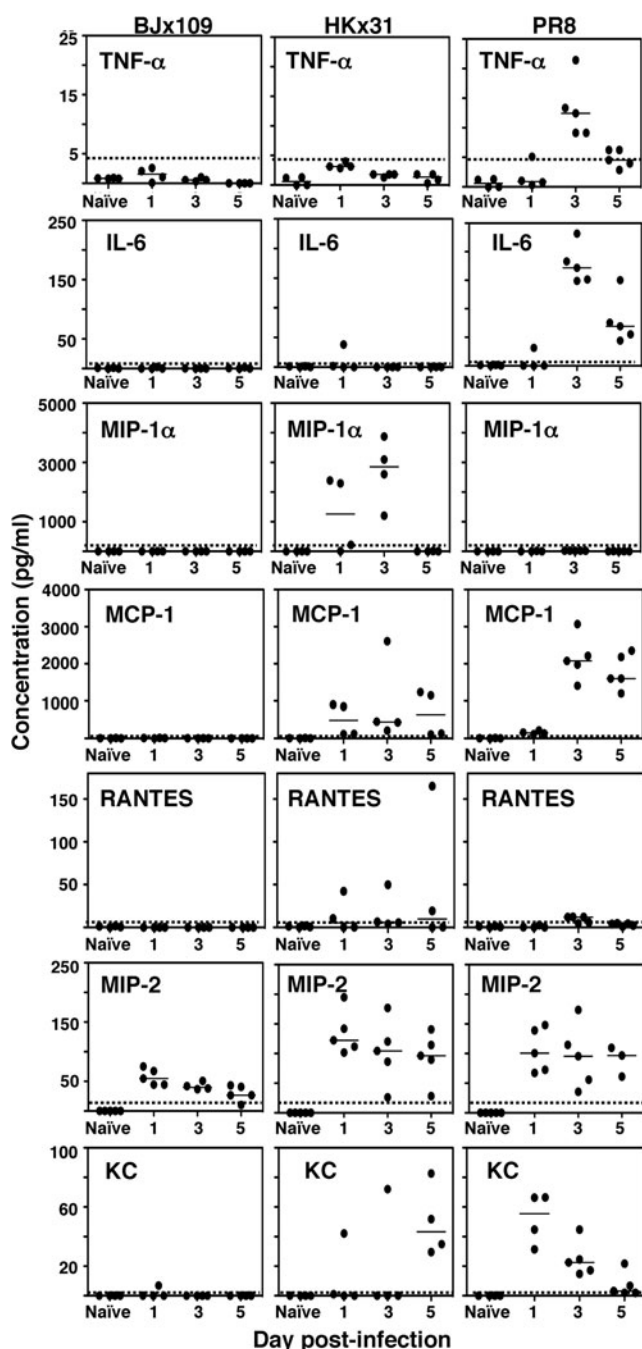
FIG. 6. Inflammatory mediators in the airways of mice infected with BJx109, HKx31, or PR8 viruses. Groups of five B6 mice were infected via the IN route with 10^5 PFU BJx109, HKx31, or PR8. Mice were euthanized at days 1, 3, and 5 post-infection, and the levels of inflammatory mediators in BAL supernatants from naïve or virus-infected mice were determined via Bio-plex assay as described in the Materials and Methods section. Results are expressed in picograms per milliliter; individual mice are indicated by black circles, and the mean is indicated by a horizontal bar. The detection limit for each mediator is indicated by a dotted line (TNF-$\alpha = 5$ pg/mL, IL-6 $= 1$ pg/mL, MIP-1$\alpha = 5$ pg/mL, MCP-1 $= 3$ pg/mL, RANTES $= 0.5$ pg/mL, MIP-2 $= 5$ pg/mL, KC $= 3$ pg/mL.

of soluble inflammatory mediators. HKx31 induced production of variable levels of MIP-1α, MCP-1, RANTES, MIP-2, and KC over the course of infection. Infection of mice with PR8 was associated with production of TNF-α, IL-6, MCP-1, KC, and MIP-2. Compared to HKx31, infection of mice with PR8 was associated with additional production of TNF-α and IL-6 during the early phase of infection. Of interest, MIP-1α, produced by airway MΦ but not AEC in response to IAV infection *in vitro* (Fig. 2), was detected in BAL fluids of HKx31-infected animals, but not PR8-infected animals.

Neutralizing activity of mouse airway fluids blocks the ability of influenza viruses to infect MΦ or AEC

BJx109 was efficient in its ability to infect both alveolar MΦ and AEC *in vitro* (Fig. 1A), yet the virus replicated poorly in mouse lungs (Fig. 4A), and few antigen-positive cells could be detected via immunoperoxidase staining (Fig. 4C). Moreover, few inflammatory mediators were induced following IN infection of mice with BJx109 (Fig. 6). The respiratory tract is lined by surfactant containing a number of proteins of the innate immune system known to mediate antiviral activity against IAV [reviewed in (12)]. Therefore, we compared the sensitivity of BJx109, HKx31, and PR8 to neutralization by cell-free BAL fluids from naïve B6 mice. Consistent with published data (57), pre-incubation of BJx109 with mouse BAL inhibited its ability to infect MDCK epithelial cells, and neutralizing activity was reversed in the presence of mannan (Fig. 7A), indicating that SP-D, rather than SP-A, was the major agent acting against BJx109. In contrast, mouse BAL exhibited weak neutralizing activity against PR8, and this was unaffected by mannan. The sensitivity of HKx31 to neutralization by mouse BAL was intermediate, between that of BJx109 and PR8.

Next, murine MΦ or AEC were pre-incubated with mouse BAL prior to the addition of either BJx109 or PR8. As seen in Fig. 7B, mouse BAL blocked infection of MΦ and AEC by BJx109, but was markedly less efficient against PR8. Again, the inhibitory activity of mouse BAL in blocking infection of MΦ and AEC by HKx31 was intermediate compared to BJx109 and PR8. Thus, mannose-binding lectins present in fluids lining the murine respiratory tract protect alveolar MΦ and AEC from infection with BJx109, but not PR8. These data are consistent with our findings that BJx109 induces high levels of chemokines and cytokines from mouse airway cells *in vitro* (Fig. 2), but not *in vivo*, following IN infection of mice (Fig. 6).

Discussion

Inflammatory mediators produced by AEC and alveolar MΦ orchestrate the cell-mediated inflammatory response elicited following respiratory infection with IAV. Moreover, the tropism of different virus strains for epithelial cells and/or MΦ is likely to determine the spectrum of chemokines and cytokines produced. In this study, BJx109, HKx31, and PR8 were shown to differ in virulence in mice, and were classified as avirulent, of intermediate virulence, and highly virulent, respectively. As BJx109 and HKx31 bear internal components derived from PR8, these differences in virulence must relate to properties of the HA/NA surface glycoproteins rather than internal components of the virion. Based on these
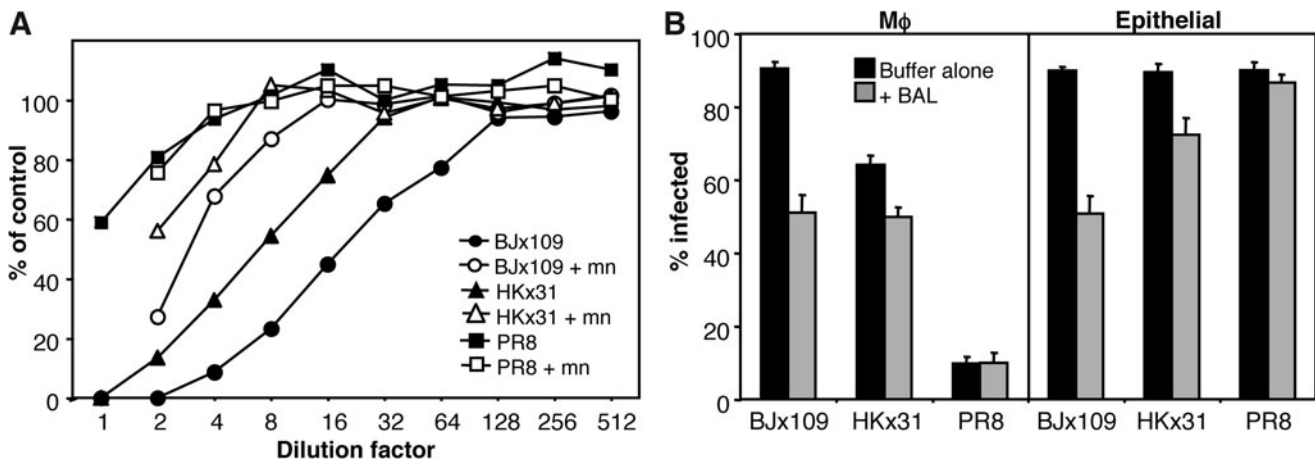
FIG. 7. Antiviral activity of mouse BAL fluids against influenza viruses. (**A**) Neutralization of IAV by a mannose-specific lectin in mouse BAL. BJx109, HKx31, and PR8 were mixed with dilutions of cell-free BAL fluid in TBS-Ca, incubated for 30 min at 37°C, and the amount of infectious virus remaining was determined by fluorescent focus assay on MDCK cell monolayers. Inhibition of neutralization was examined by the addition of mannan (mn; to a final concentration of 10 mg/mL) to BAL 30 min prior to the addition of virus. (**B**) Ability of mouse BAL to inhibit infection of MΦ and epithelial cells. Mouse BAL or buffer alone was added to monolayers of MΦ or LA-4 mouse epithelial cells and incubated at 37°C for 5 min, prior to the addition of 1×10^6 PFU of BJx109, HKx31, or PR8. After 1 h, the monolayers were washed, incubated 8 h, and then fixed and stained by immunofluorescence for expression of newly-synthesized NP viral protein. Data represent the mean percent infection (± 1 SD) from a minimum of four independent fields per chamber.

findings, we investigated factors that contribute to the virulence of PR8 in mice. In particular, PR8 did not elicit innate responses from airway MΦ *in vitro,* and was resistant to neutralization by mouse airway fluids. Moreover, PR8 was shown to replicate and spread throughout the lung, inducing severe viral pneumonia. Together these data indicate that the ability of PR8 to evade components of innate immune defense is likely to be an important factor contributing to its virulence in mice.

The ability of BJx109, HKx31, and PR8 to infect airway MΦ correlated with their ability to induce inflammatory mediators from these cells. Accordingly, BJx109 was a potent inducer of inflammatory mediators (TNF-α, MIP-1α, RANTES, MIP-2, and KC) from airway MΦ, whereas PR8 was not (Fig. 2). Mouse airway MΦ produce TNF-α, but not MCP-1, in response to IAV (24), and IAV-infected airway MΦ from pigs produced IL-1β, IL-6, IL-8, and TNF-α (51). however, most *invitro* studies have utilized human monocytes/MΦ. In contrast to mouse MΦ, human MΦ exposed to PR8 secreted a range of inflammatory mediators, including IL-1β, IL-6, TNF-α, MIP-1α, MCP-1, and RANTES (7,17,25,43,54). Sialic acid is the primary attachment receptor for IAV on target cells [reviewed by (52)], and human airway MΦ express predominantly α(2,3)-Gal-linked sialic acid (39,40). In contrast, we have found α(2,6)-Gal-linked sialic acid to be the major linkage expressed by mouse airway MΦ (56). The preference of PR8 for α(2,3)-Gal-linked sialic acid (55,62) is consistent with its ability to infect human, but not mouse, MΦ. Furthermore, in contrast to mouse MΦ, some human MΦ have been reported to support productive IAV infection (42), suggesting that human and mouse MΦ differ in their ability to recognize and respond to IAV.

Mouse AEC exposed to BJx109, HKx31, or PR8 produced MCP-1, RANTES, MIP-2, and KC, as well as some TNF-α and IL-6 (Fig. 2). These findings are consistent with previous re-

ports of IAV-induced production of TNF-α, IL-6, and type I IFN from murine tracheal epithelial cells (38), and PR8-induced secretion of MCP-1 and RANTES from mouse AEC (24). Human AEC exposed to IAV produce RANTES, MCP-1, and IL-8 (2,29), as well as IP-10, IL-6, and IFN-β (8–10). Based on *in vitro* studies, it has been proposed that human AEC secrete only neutrophil-attracting chemokines (such as IL-8) in response to IAV, whereas human MΦ secrete mononuclear leukocyte-attracting chemokines, and actually suppress neutrophil-attracting chemoattractants (2,29,53). KC/MIP-2, functional homologues of human IL-8 (5,60), were produced by mouse AEC in response to IAV (Fig. 2), and by mouse airway MΦ in response to BJx109 and HKx31 (Fig. 2). Thus, mouse airway cells (AEC and MΦ) do not display the polarized cytokine/chemokine profiles reported following exposure of human cells to IAV.

To better understand influenza-induced disease in mice, we characterized IAV-induced cytokine and chemokine production *in vivo*. BJx109, HKx31, and PR8 induced mild, moderate, and severe disease, respectively (Fig. 3). *In vitro*, BJx109, HKx31, and PR8 infected AEC to equivalent levels (Fig. 1A), yet *in vivo* BJx109 replicated poorly, and few IAV-positive cells were detected in the lung (Fig. 4C). Thus caution must be exercised in extrapolating *in vitro* observations to the complex microenvironment of the lung. *In vivo*, respiratory epithelium is lined by pulmonary surfactant, a rich source of proteins of the innate immune system that mediate antiviral activity against IAV (19,22,45). Mouse BAL inhibited the ability of BJx109, but not PR8, to infect mouse AEC and MΦ (Fig. 7B), a finding consistent with reports that PR8 is resistant to neutralization by SP-D (20,45). These results suggest that BJx109 is neutralized by SP-D in lung fluids before it can infect the respiratory epithelium, and are consistent with our findings that BJx109 induced high levels of inflammatory mediators from airway MΦ

in vitro, yet levels in BAL were very low or below the level of detection.

Infection of mice with PR8 led to rapid weight loss and disease (Fig. 3), associated with extensive virus replication and spread in the lungs (Fig. 4), and pulmonary inflammation and damage to lung epithelium (Fig. 5). Several independent studies have reported a rise in the levels of inflammatory mediators (e.g., TNF-α, IL-1α, IL-1β, IL-6, and MCP-1) in BAL or lung homogenates in temporal association with the development of symptoms and lung pathology (23,32,41). In contrast to the protective responses elicited in BJx109- and HKx31-infected mice, PR8 infection was associated with progressive accumulation of leukocytes, leading to lung inflammation and pulmonary edema (Fig. 5). These hallmark features of acute respiratory distress syndrome (ARDS) have previously been associated with severe disease in mice infected with H5N1 (67) or H9N2 (14) viruses, and in influenza virus–infected mice in which specific components of the immune response have been depleted (58,59). The failure of PR8 to elicit innate responses from alveolar MΦ, and its resistance to mouse BAL, favor immediate infection and replication in AEC in the early phase of infection. Once PR8 infection is established, continued replication and amplification of virus results in tissue damage; the high levels of chemokines and cytokines that we observed in BAL from PR8-infected mice (Fig. 6) are consistent with previous findings (6,23,64). BJx109, HKx31, and PR8 did not differ in their ability to replicate in mouse AEC *in vitro* (Fig. 1B), indicating that the different virus loads observed in mouse lungs (Fig. 4A) reflect differences in susceptibility to innate defenses rather than intrinsic differences in the ability to infect and replicate in AEC. The poor ability of PR8 to infect airway MΦ, and its weak sensitivity to innate proteins in BAL, are consistent with high levels of virus growth in mouse lungs.

BJx109, HKx31, and PR8 share internal components derived from PR8, but differ in HA/NA, and thus in sensitivity to components of innate host defense. BJx109 grows poorly in the airways of immunocompetent mice, but can replicate to high titers in mice depleted of airway MΦ (59). PR8 grows to high titers in mouse lungs, is unaffected by depletion of airway MΦ (59), and is resistant to neutralization by mouse BAL (Fig. 7) (57). BJx109 and HKx31 elicited similar levels of cytokines and chemokines from airway MΦ *in vitro* (Fig. 2), yet BJx109 was markedly more sensitive to inhibition by airway fluids (Fig. 7). The differential sensitivity of BJx109 and HKx31 to inhibitory proteins in the airways might be an important factor contributing to their differential virulence, particularly in B6.RAG-1$^{-/-}$ mice lacking T-cell– and B-cell–mediated immunity.

Experiments to delineate the relative contribution of SP-D and airway MΦ to innate defense against IAV are complicated, as their production and regulation in the airways are intimately related. For example, impaired surfactant catabolism by airway MΦ can result in alveolar proteinosis [reviewed in (11,26)]. Moreover, researchers have used knockout mice to demonstrate the importance of SP-D in limiting replication of highly glycosylated IAV (22,34,63); however, interpretation is complicated by the aberrant pulmonary homeostasis in SP-D-deficient mice, which includes MΦ activation and surfactant phospholipid accumulations (27,28,31). In our studies, infection of mouse MΦ and epithelial cells was also modulated in the presence of BAL (Fig. 7). The intimate association of sur-

factant and airway MΦ therefore appears important in mediating coordinated control of IAV by the innate immune system. SP-D in surfactant and MMR on airway MΦ are soluble and cell-associated C-type lectins that recognize glycans on HA/NA to destroy IAV. The ability of PR8 to avoid detection by C-type lectins of the innate immune system is likely an important factor contributing to its virulence.

Acknowledgments

Author Disclosure Statement

M.D.T. carried out the majority of experiments described in this study, analyzed and interpreted data, and prepared figures for the manuscript. H.C.S. prepared the primary mouse airway epithelial cell cultures used in this study. P.C.R. and M.D.T. designed the study, and P.C.R. wrote the manuscript. A.G.B. contributed to interpretation of the data and the writing of the manuscript. All authors read and approved the final manuscript. The authors declare that no conflicting financial interests exist.

References

1. Anders EM, Hartley CA, Reading PC, and Ezekowitz RA: Complement-dependent neutralization of influenza virus by a serum mannose-binding lectin. J Gen Virol 1994;75(Pt 3):615–622.

2. Arndt U, Wennemuth G, Barth P, *et al.*: Release of macrophage migration inhibitory factor and CXCL8/interleukin-8 from lung epithelial cells rendered necrotic by influenza A virus infection. J Virol 2002;76:9298–9306.

3. Bender BS, and Small PA Jr: Influenza: pathogenesis and host defense. Semin Respir Infect 1992;7:38–45.

4. Benne CA, Kraaijeveld CA, van Strijp JA, *et al.*: Interactions of surfactant protein A with influenza A viruses: binding and neutralization. J Infect Dis 1995;171:335–341.

5. Bozic CR, Gerard NP, von Uexkull-Guldenband C, *et al.*: The murine interleukin 8 type B receptor homologue and its ligands. Expression and biological characterization. J Biol Chem 1994;269:29355–29358.

6. Buchweitz JP, Harkema JR, and Kaminski NE: Time-dependent airway epithelial and inflammatory cell responses induced by influenza virus A/PR/8/34 in C57BL/6 mice. Toxicol Pathol 2007;35:424–435.

7. Bussfeld D, Kaufmann A, Meyer RG, Gemsa D, and Sprenger H: Differential mononuclear leukocyte attracting chemokine production after stimulation with active and inactivated influenza A virus. Cell Immunol 1998;186:1–7.

8. Chan MC, Chan RW, Yu WC, *et al.*: Influenza H5N1 virus infection of polarized human alveolar epithelial cells and lung microvascular endothelial cells. Respir Res 2009;10:102.

9. Chan MC, Cheung CY, Chui WH, *et al.*: Proinflammatory cytokine responses induced by influenza A (H5N1) viruses in primary human alveolar and bronchial epithelial cells. Respir Res 2005;6:135.

10. Chan RW, Yuen KM, Yu WC, Ho CC, Nicholls JM, Peiris JS, and Chan MC: Influenza H5N1 and H1N1 virus replication and innate immune responses in bronchial epithelial cells are influenced by the state of differentiation. PLoS One 2010;5:e8713.

11. Chroneos ZC, Sever-Chroneos Z, and Shepherd VL: Pulmonary surfactant: an immunological perspective. Cell Physiol Biochem 2010;25:13–26.

12. Crouch E, and Wright JR: Surfactant proteins a and d and pulmonary host defense. Annu Rev Physiol 2001;63:521–554.

13. Davidson DJ, Kilanowski FM, Randell SH, Sheppard DN, and Dorin JR: A primary culture model of differentiated murine tracheal epithelium. Am J Physiol Lung Cell Mol Physiol 2000;279:L766–L778.

14. Deng G, Bi J, Kong F, et al.: Acute respiratory distress syndrome induced by H9N2 virus in mice. Arch Virol 2010; 155:187–195.

15. Forrest IA, Murphy DM, Ward C, et al.: Primary airway epithelial cell culture from lung transplant recipients. Eur Respir J 2005;26:1080–1085.

16. Fujisawa H, Tsuru S, Taniguchi M, Zinnaka Y, and Nomoto K: Protective mechanisms against pulmonary infection with influenza virus. I. Relative contribution of polymorphonuclear leukocytes and of alveolar macrophages to protection during the early phase of intranasal infection. J Gen Virol 1987;68(Pt 2):425–432.

17. Gong JH, Sprenger H, Hinder F, et al.: Influenza A virus infection of macrophages. Enhanced tumor necrosis factor-alpha (TNF-alpha) gene expression and lipopolysaccharide-triggered TNF-alpha release. J Immunol 1991;147:3507–3513.

18. Hartshorn K, Chang D, Rust K, White M, Heuser J, and Crouch E: Interactions of recombinant human pulmonary surfactant protein D and SP-D multimers with influenza A. Am J Physiol 1996;271:L753–L762.

19. Hartshorn KL, Crouch EC, White MR, Eggleton P, Tauber AI, Chang D, and Sastry K: Evidence for a protective role of pulmonary surfactant protein D (SP-D) against influenza A viruses. J Clin Invest 1994;94:311–319.

20. Hartshorn KL, White MR, Shepherd V, Reid K, Jensenius JC, and Crouch EC: Mechanisms of anti-influenza activity of surfactant proteins A and D: comparison with serum collectins. Am J Physiol 1997;273:L1156–L1166.

21. Hashimoto Y, Moki T, Takizawa T, Shiratsuchi A, and Nakanishi Y: Evidence for phagocytosis of influenza virus-infected, apoptotic cells by neutrophils and macrophages in mice. J Immunol 2007;178:2448–2457.

22. Hawgood S, Brown C, Edmondson J, et al.: Pulmonary collectins modulate strain-specific influenza a virus infection and host responses. J Virol 2004;78:8565–8572.

23. Hennet T, Ziltener HJ, Frei K, and Peterhans E: A kinetic study of immune mediators in the lungs of mice infected with influenza A virus. J Immunol 1992;149:932–939.

24. Herold S, von Wulffen W, Steinmueller M, et al.: Alveolar epithelial cells direct monocyte transepithelial migration upon influenza virus infection: impact of chemokines and adhesion molecules. J Immunol 2006;177:1817–1824.

25. Hofmann P, Sprenger H, Kaufmann A, Bender A, Hasse C, Nain M, and Gemsa D: Susceptibility of mononuclear phagocytes to influenza A virus infection and possible role in the antiviral response. J Leukoc Biol 1997;61: 408–414.

26. Huizar I, and Kavuru MS: Alveolar proteinosis syndrome: pathogenesis, diagnosis, and management. Curr Opin Pulm Med 2009;15:491–498.

27. Ikegami M, Na CL, Korfhagen TR, and Whitsett JA: Surfactant protein D influences surfactant ultrastructure and uptake by alveolar type II cells. Am J Physiol Lung Cell Mol Physiol 2005;288:L552–L561.

28. Ikegami M, Whitsett JA, Jobe A, Ross G, Fisher J, and Korfhagen T: Surfactant metabolism in SP-D gene-targeted mice. Am J Physiol Lung Cell Mol Physiol 2000;279:L468–L476.

29. Julkunen I, Melen K, Nyqvist M, Pirhonen J, Sareneva T, and Matikainen S: Inflammatory responses in influenza A virus infection. Vaccine 2000;19(Suppl 1):S32–S37.

30. Kim HM, Lee YW, Lee KJ, et al.: Alveolar macrophages are indispensable for controlling influenza viruses in lungs of pigs. J Virol 2008;82:4265–4274.

31. Korfhagen TR, Sheftelyevich V, Burhans MS, et al.: Surfactant protein-D regulates surfactant phospholipid homeostasis in vivo. J Biol Chem 1998;273:28438–28443.

32. Kurokawa M, Imakita M, Kumeda CA, and Shiraki K: Cascade of fever production in mice infected with influenza virus. J Med Virol 1996;50:152–158.

33. LeVine AM, Hartshorn K, Elliott J, Whitsett J, and Korfhagen T: Absence of SP-A modulates innate and adaptive defense responses to pulmonary influenza infection. Am J Physiol Lung Cell Mol Physiol 2002;282:L563–L572.

34. LeVine AM, Whitsett JA, Hartshorn KL, Crouch EC, and Korfhagen TR: Surfactant protein D enhances clearance of influenza A virus from the lung in vivo. J Immunol 2001; 167:5868–5873.

35. Li G, Siddiqui J, Hendry M, et al.: Surfactant protein-A–deficient mice display an exaggerated early inflammatory response to a beta-resistant strain of influenza A virus. Am J Respir Cell Mol Biol 2002;26:277–282.

36. Matikainen S, Pirhonen J, Miettinen M, Lehtonen A, Govenius-Vintola C, Sareneva T, and Julkunen I: Influenza A and Sendai viruses induce differential chemokine gene expression and transcription factor activation in human macrophages. Virology 2000;276:138–147.

37. Mombaerts P, Iacomini J, Johnson RS, Herrup K, Tonegawa S, and Papaioannou VE: RAG-1-deficient mice have no mature B and T lymphocytes. Cell 1992;68:869–877.

38. Newby CM, Sabin L, and Pekosz A: The RNA binding domain of influenza A virus NS1 protein affects secretion of tumor necrosis factor alpha, interleukin-6, and interferon in primary murine tracheal epithelial cells. J Virol 2007;81: 9469–9480.

39. Nicholls JM, Bourne AJ, Chen H, Guan Y, and Peiris JS: Sialic acid receptor detection in the human respiratory tract: evidence for widespread distribution of potential binding sites for human and avian influenza viruses. Respir Res 2007;8:73.

40. Nicholls JM, Peiris JS, and Guan Y: Sialic acid and receptor expression on the respiratory tract in normal subjects and H5N1 and non-avian influenza patients. Hong Kong Med J 2009;15:16–20.

41. Peper RL, and Van Campen H: Tumor necrosis factor as a mediator of inflammation in influenza A viral pneumonia. Microb Pathog 1995;19:175–183.

42. Perrone LA, Plowden JK, Garcia-Sastre A, Katz JM, and Tumpey TM: H5N1 and 1918 pandemic influenza virus infection results in early and excessive infiltration of macrophages and neutrophils in the lungs of mice. PLoS Pathog 2008;4:e1000115.

43. Peschke T, Bender A, Nain M, and Gemsa D: Role of macrophage cytokines in influenza A virus infections. Immunobiology 1993;189:340–355.

44. Reading PC, Miller JL, and Anders EM: Involvement of the mannose receptor in infection of macrophages by influenza virus. J Virol 2000;74:5190–5197.

45. Reading PC, Morey LS, Crouch EC, and Anders EM: Collectin-mediated antiviral host defense of the lung: evidence from influenza virus infection of mice. J Virol 1997;71:8204–8212.

46. Reading PC, Pickett DL, Tate MD, Whitney PG, Job ER, and Brooks AG: Loss of a single N-linked glycan from the hemagglutinin of influenza virus is associated with resistance to collectins and increased virulence in mice. Respir Res 2009;10:117.

47. Reading PC, Whitney PG, Pickett DL, Tate MD, and Brooks AG: Influenza viruses differ in ability to infect macrophages and to induce a local inflammatory response following intraperitoneal injection of mice. Immunol Cell Biol 2010; 88:641–650.

48. Rodgers B, and Mims CA: Interaction of influenza virus with mouse macrophages. Infect Immun 1981;31:751–757.

49. Ronni T, Matikainen S, Sareneva T, Melen K, Pirhonen J, Keskinen P, and Julkunen I: Regulation of IFN-alpha/beta, MxA, 2′,5′-oligoadenylate synthetase, and HLA gene expression in influenza A-infected human lung epithelial cells. J Immunol 1997;158:2363–2374.

50. Roper JM, Staversky RJ, Finkelstein JN, Keng PC, and O'Reilly MA: Identification and isolation of mouse type II cells on the basis of intrinsic expression of enhanced green fluorescent protein. Am J Physiol Lung Cell Mol Physiol 2003;285:L691–L700.

51. Seo SH, Webby R, and Webster RG: No apoptotic deaths and different levels of inductions of inflammatory cytokines in alveolar macrophages infected with influenza viruses. Virology 2004;329:270–279.

52. Skehel JJ, and Wiley DC: Receptor binding and membrane fusion in virus entry: the influenza hemagglutinin. Annu Rev Biochem 2000;69:531–569.

53. Sprenger H, Kaufmann A, Garn H, Lahme B, Gemsa D, and Gressner AM: Induction of neutrophil-attracting chemokines in transforming rat hepatic stellate cells. Gastroenterology 1997;113:277–285.

54. Sprenger H, Meyer RG, Kaufmann A, Bussfeld D, Rischkowsky E, and Gemsa D: Selective induction of monocyte and not neutrophil-attracting chemokines after influenza A virus infection. J Exp Med 1996;184:1191–1196.

55. Suzuki Y, Nagao Y, Kato H, Matsumoto M, Nerome K, Nakajima K, and Nobusawa E: Human influenza A virus hemagglutinin distinguishes sialyloligosaccharides in membrane-associated gangliosides as its receptor which mediates the adsorption and fusion processes of virus infection. Specificity for oligosaccharides and sialic acids and the sequence to which sialic acid is attached. J Biol Chem 1986;261:17057–17061.

56. Tate MD, Brooks AG, and Reading PC: Correlation between sialic acid expression and infection of murine macrophages by different strains of influenza virus. Microb Infect 2010; [Epub ahead of print].

57. Tate MD, Brooks AG, and Reading PC: Inhibition of lectin-mediated innate host defences in vivo modulates disease severity during influenza virus infection. Immunol Cell Biol 2010; [Epub ahead of print].

58. Tate MD, Deng YM, Jones JE, Anderson GP, Brooks AG, and Reading: Neutrophils ameliorate lung injury and the development of severe disease during influenza infection. J Immunol 2009;183:7441–7450.

59. Tate MD, Pickett DL, van Rooijen N, Brooks AG, and Reading PC: Critical role of airway macrophages in modulating disease severity during influenza virus infection of mice. J Virol 2010;84:7569–7580.

60. Tekamp-Olson P, Gallegos C, Bauer D, et al.: Cloning and characterization of cDNAs for murine macrophage inflammatory protein 2 and its human homologues. J Exp Med 1990;172:911–919.

61. Tumpey TM, Garcia-Sastre A, Taubenberger JK, et al.: Pathogenicity of influenza viruses with genes from the 1918 pandemic virus: functional roles of alveolar macrophages and neutrophils in limiting virus replication and mortality in mice. J Virol 2005;79:14933–14944.

62. van Eijk M, White MR, Batenburg JJ, Vaandrager AB, van Golde LM, Haagsman HP, and Hartshorn KL: Interactions of influenza A virus with sialic acids present on porcine surfactant protein D. Am J Respir Cell Mol Biol 2004;30:871–879.

63. Vigerust DJ, Ulett KB, Boyd KL, Madsen J, Hawgood S, and McCullers JA: N-linked glycosylation attenuates H3N2 influenza viruses. J Virol 2007;81:8593–8600.

64. Wareing MD, Lyon AB, Lu B, Gerard C, and Sarawar SR: Chemokine expression during the development and resolution of a pulmonary leukocyte response to influenza A virus infection in mice. J Leukoc Biol 2004;76:886–895.

65. Wells MA, Albrecht P, Daniel S, and Ennis FA: Host defense mechanisms against influenza virus: interaction of influenza virus with murine macrophages in vitro. Infect Immun 1978;22:758–762.

66. Wijburg OL, DiNatale S, Vadolas J, van Rooijen N, and Strugnell RA: Alveolar macrophages regulate the induction of primary cytotoxic T-lymphocyte responses during influenza virus infection. J Virol 1997;71:9450–9457.

67. Xu T, Qiao J, Zhao L, et al.: Acute respiratory distress syndrome induced by avian influenza A (H5N1) virus in mice. Am J Respir Crit Care Med 2006;174:1011–1017.

Address correspondence to:
Dr. Patrick C. Reading
Department of Microbiology and Immunology
University of Melbourne
Royal Parade
Victoria, 3010, Australia

E-mail: preading@unimelb.edu.au